doi:10.1038/nature12328

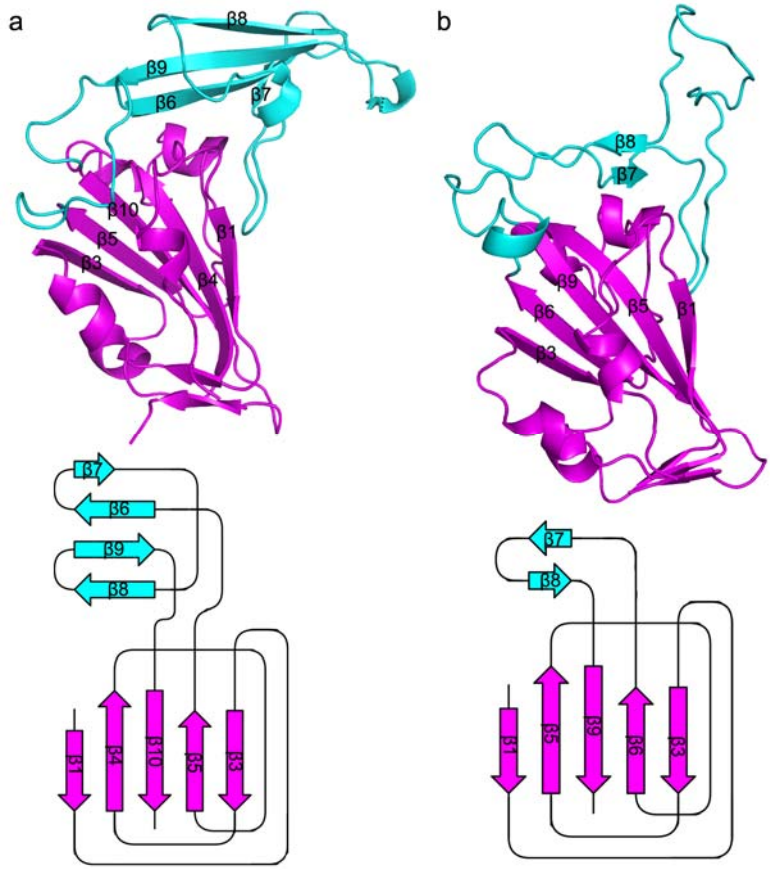

Supplementary Figure 1: Topological comparison of the RBD external subdomain between MERS-CoV and SARS-CoV. Top panel: A ribbon representation of the crystal structure. Bottom panel: A schematic view of the RBD topology. For clarity, only strands (drawn as arrows) are presented and labeled. The core and external subdomains are colored magenta and cyan, respectively. **a**, MERS-CoV RBD. **b**, SARS-CoV RBD (PDB code: 2dd8).

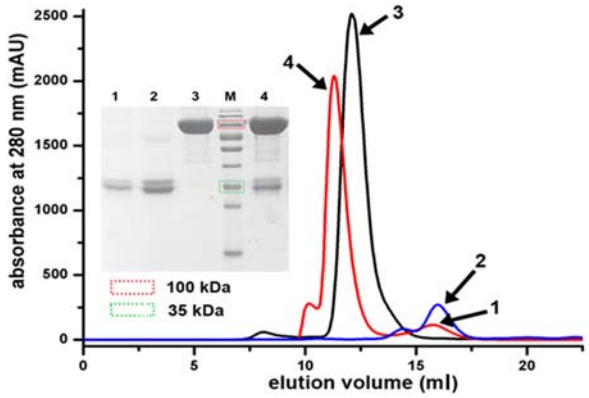

Supplementary Figure 2: Size exclusion analysis of MERS-CoV RBD (blue), CD26 (black) and the RBD-CD26 complex (red). The three prepared samples were loaded on a calibrated Superdex® 200 column (10/300 GL) individually, and the overlaid chromatographs are shown. The SDS-PAGE migration profiles of the pooled samples (1-4) are also presented in the figure, with the 35 and 100 kDa molecular weight standards being highlighted. Clearly shown is that *in vitro* mixture of MERS-CoV RBD and CD26 could yield a stable complex.

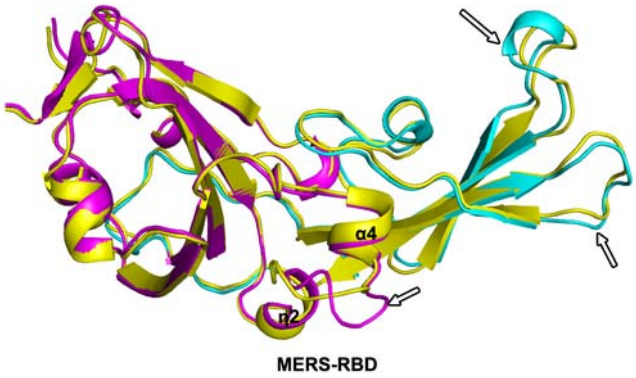

Supplementary Figure 3: Superimposition of the MERS-CoV RBD structure for the free and the receptor-bounded forms. Structural variances are observed for the tip-loops in the external subdomain and the η2-α4 loop in the core subdomain, which are marked with arrows. Magenta: free RBD, core subdomain; cyan: free RBD, external subdomain; yellow: the bound RBD.

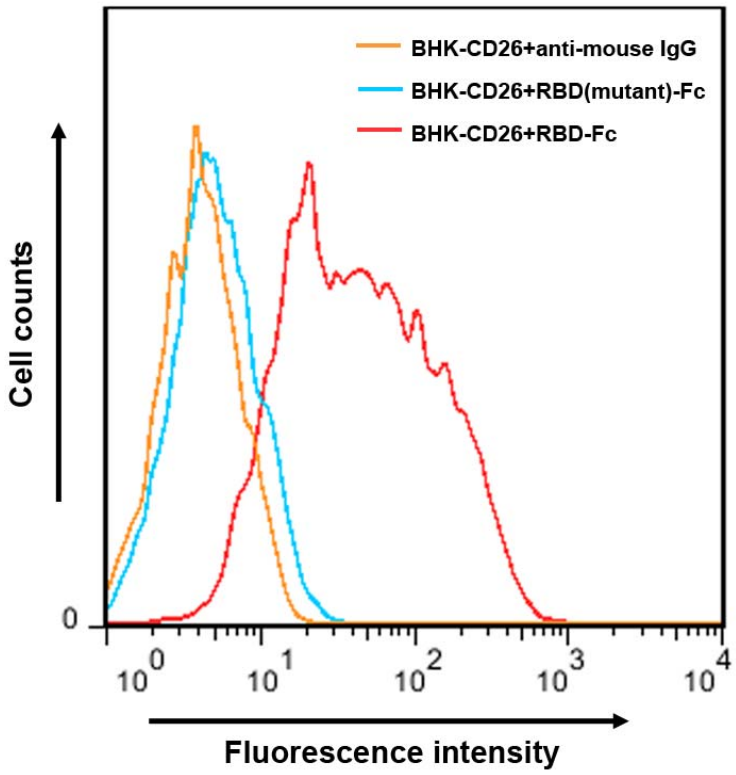

Supplementary Figure 4: A flowcytometric assay characterizing the binding of mutant RBD to CD26. The identified hydrophilic residues involved in CD26 engagement are mutated as specified in the Methods. The resultant mutant RBD-Fc was compared to the wild type RBD-Fc for CD26 binding. The profiles are shown, with the mutations clearly abrogating the binding.

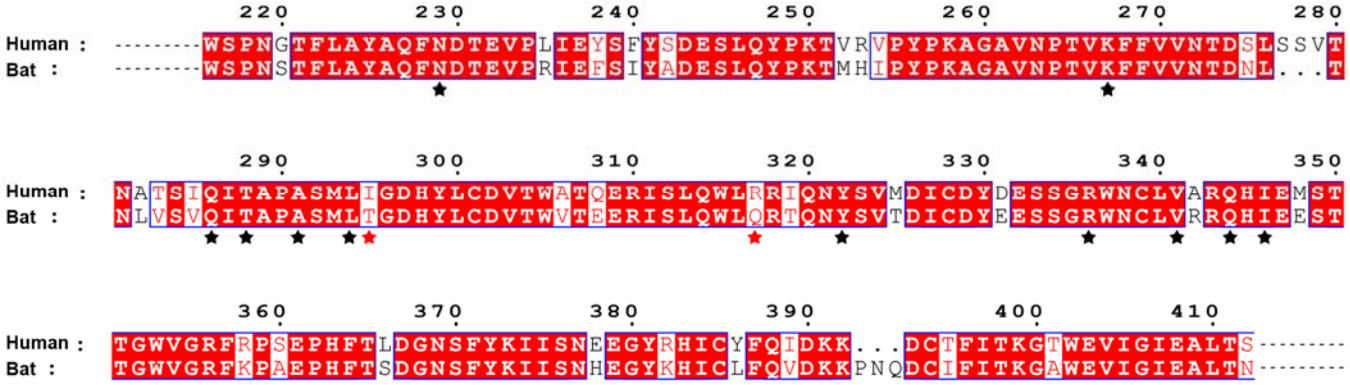

Supplementary Figure 5: Amino acid sequence alignment between human- and bat-CD26 highlighting the MERS-CoV RBD binding sites. The identified key-binding residues are marked with stars. Black stars indicate those amino acids that are conserved between human and bat, while red stars highlight those that are of variance. Accession codes: human CD26 (NP_001926); bat CD26 (Uniprot, K9J2R0).

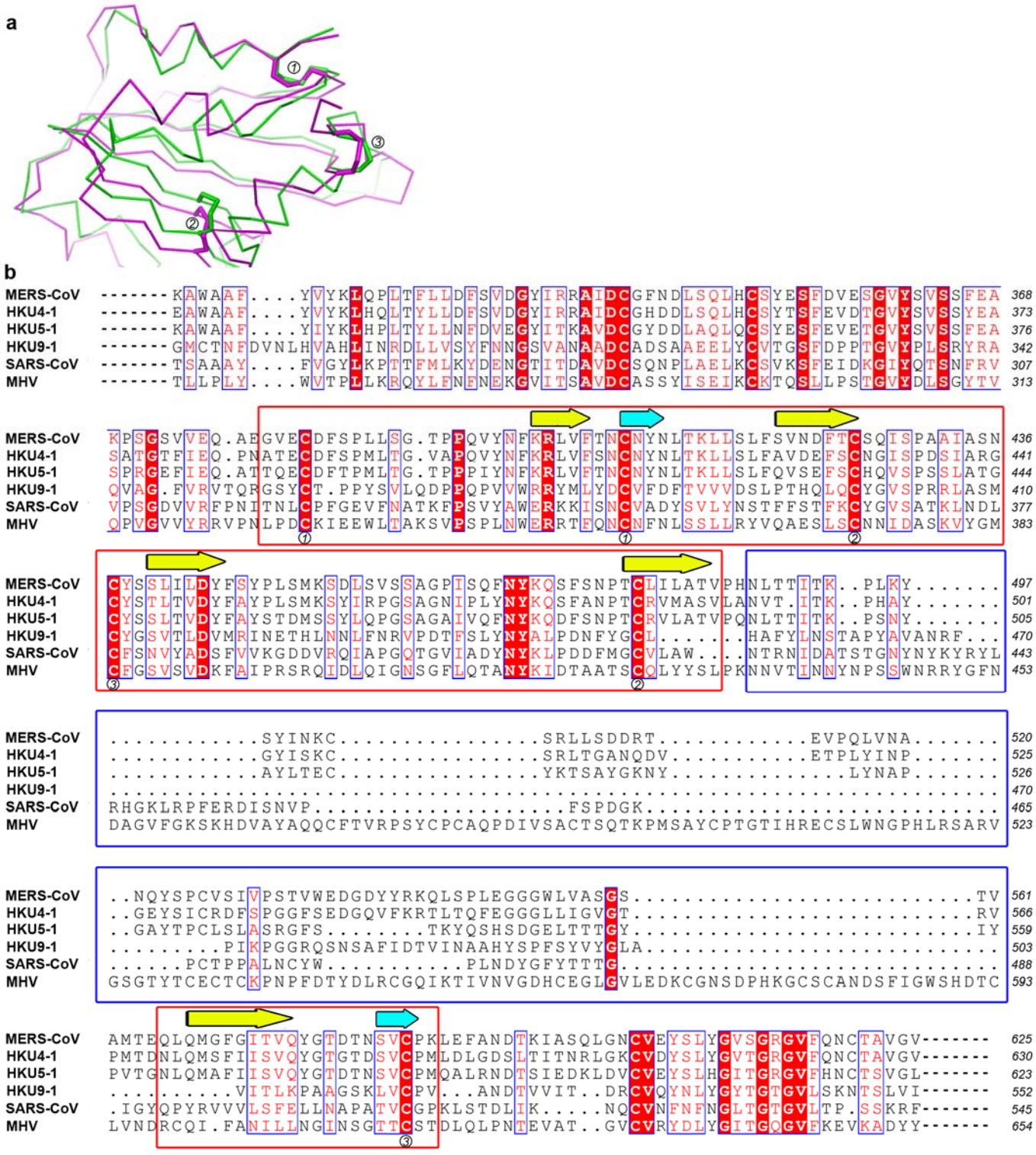

Supplementary Figure 6: Comparison of the RBD or the RBD-homologous regions among typical betacoronavirus members. a, Steric conservation of the core-subdomain-related disulphide bonds between MERS-CoV (magenta) and

SARS-CoV (green) RBDs. The structures shown in ribbon are superimposed onto each other, and the three disulphide bonds shown as sticks are highlighted and labeled. **b,** Alignment of the spike amino acid sequences from typical betacoronaviruses highlighting the RBD-homologous regions. Based on the structure of MERS-CoV RBD, the core- and external-subdomain regions are encircled with red and blue boxes, respectively. Those strands forming the center sheet of the core are marked with yellow arrows, and the strands clinching the RBD termini are indicated with cyan arrows. The conserved cysteine residues are labeled. Residue numberings are based on the full-length proteins. Abbreviations and accession codes: MERS-CoV (Middle East respiratory syndrome coronavirus, JX869059); HKU4-1 (bat coronavirus HKU4-1, EF065505); HKU5-1 (bat coronavirus HKU5-1, EF065509); HKU9-1 (bat coronavirus HKU9-1, EF065513); SARS-CoV (severe acute respiratory syndrome coronavirus, NC_004718) and MHV (murine hepatitis virus, NC_006852).

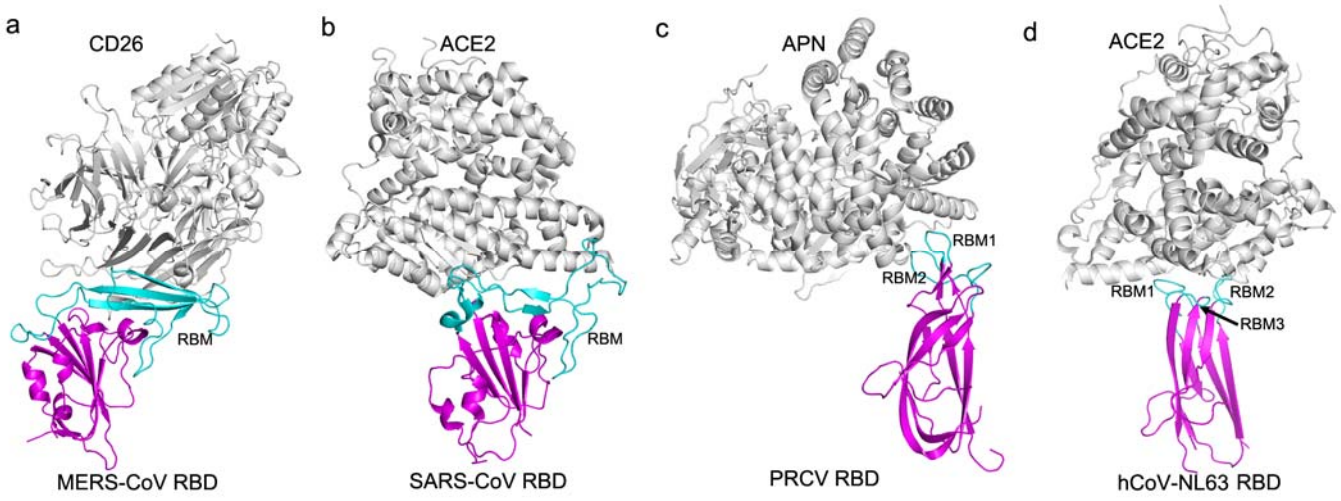

Supplementary Figure 7: Structural comparison of the virus-S-receptor complexes in *Coronaviridae* family. The receptors are shown in gray color, and the virus RBDs are highlighted in magenta for the core-subdomain and in cyan for the receptor binding motifs (RBMs). **a**, MERS-CoV RBD bound to human CD26. **b**, SARS-CoV RBD bound to human ACE2 (PDB code: 2AJF). **c**, PRCV (porcine respiratory coronavirus) RBD bound to porcine APN (PDB code: 4F5C). **d**, hCoV-NL63 (human coronavirus NL63) RBD bound to human ACE2 (PDB code: 3KBH).

Supplementary Table 1. Crystallographic data collection and refinement statistics

	RBD	Au derivative RBD	RBD-CD26
Data collection			
Space group	P212121	P212121	P6122
Cell dimensions			
a, *b*, *c* (Å)	46.98, 108.47, 125.93	46.58, 107.19, 126.39	110.22, 110.22, 527.60
α, β, γ (°)	90, 90, 90	90, 90, 90	90, 90, 120
		Peak	
Resolution (Å)	50-2.50(2.59-2.50)	50-3.00(3.11-3.00)	50-2.70(2.80-2.70)
R_{merge}	0.095(0.659)	0.149(0.679)	0.115(0.639)
$I / \sigma I$	21.6(4.3)	24.2(6.5)	18.7(3.7)
Completeness (%)	99.8(100.0)	99.8(100.0)	99.9(100.0)
Redundancy	7.7(8.2)	10.4(10.9)	7.6(7.9)
Refinement			
Resolution (Å)	49.81-2.51		48.85-2.70
No. reflections	22479		53432
R_{work} / R_{free}	0.2079/0.2509		0.1982/0.2324
No. atoms			
Protein	3244		7751
Ligand/ion	0		0
Water	63		194
B-factors			
Protein	64.5		54.2
Ligand/ion	0		0
Water	49.1		46.3
R.m.s. deviations			
Bond lengths (Å)	0.005		0.006
Bond angles (°)	0.936		1.028

*In each case, a single crystal was used to collect the data. Values in parentheses are for the highest-resolution shell.